The cerebellar mossy fiber synapse as a model for high-frequency transmission in the mammalian CNS

Delvendahl, Igor ; Hallermann, Stefan

Abstract: The speed of neuronal information processing depends on neuronal firing frequency. Here, we describe the evolutionary advantages and ubiquitous occurrence of high-frequency firing within the mammalian nervous system in general. The highest firing frequencies so far have been observed at the cerebellar mossy fiber to granule cell synapse. The mechanisms enabling high-frequency transmission at this synapse are reviewed and compared with other synapses. Finally, information coding of high-frequency signals at the mossy fiber synapse is discussed. The exceptionally high firing frequencies and amenability to high-resolution technical approaches both in vitro and in vivo establish the cerebellar mossy fiber synapse as an attractive model to investigate high-frequency signaling from the molecular up to the network level.

DOI: https://doi.org/10.1016/j.tins.2016.09.006

Title: The cerebellar mossy fiber synapse as a model for high-frequency transmission in the mammalian CNS

Authors: Igor Delvendahl[1,2] and Stefan Hallermann[1,*]

Affiliation: [1] Carl-Ludwig-Institute for Physiology, Medical Faculty, University of Leipzig, Liebigstr. 27, 04103 Leipzig, Germany.

[2] Present address: Institute for Molecular Life Sciences, University of Zurich, Winterthurerstrasse 190, 8057 Zurich, Switzerland.

* Correspondence: hallermann@medizin.uni-leipzig.de

Short title: High-frequency synaptic transmission

Keywords: Synapse; Synaptic transmission; Cerebellum; High-frequency signaling

Abstract

The speed of neuronal information processing depends on neuronal firing frequency. Here, we describe the evolutionary advantages and ubiquitous occurrence of high-frequency firing within the mammalian nervous system in general. The highest firing frequencies so far have been observed at the cerebellar mossy fiber to granule cell KILL (GC) synapse. The mechanisms enabling high-frequency transmission at this synapse are reviewed and compared with other synapses. Finally, information coding of high-frequency signals at the mossy fiber synapse is discussed. The exceptionally high firing frequencies and amenability to high-resolution technical approaches both *in vitro* and *in vivo* establish the cerebellar mossy fiber synapse as an attractive model to investigate high-frequency signaling from the molecular up to the network level.

Advantages and disadvantages of high-frequency rate coding

The capacity for rapid information processing in the mammalian nervous system has been optimized by natural selection. As a consequence, processing of, e.g., sensory afferents from whiskers [1] or the cochlea [2] features a temporal precision in the microsecond range in response to specific stimuli. A variety of neuronal mechanisms evolved to process information rapidly. Here, we focus on the amazing ability of neurons to fire trains of action potentials (APs) and transmit information at high frequency (defined as frequencies well above 100 Hz). Other mechanisms, such as a rapid axonal AP conduction and short synaptic delay, are also essential for rapid information processing but will not be addressed in detail. We argue that high-frequency transmission has evolutionary advantages (Figure 1) and occurs ubiquitously in the mammalian central nervous system (CNS, Figure 2). We further suggest that the cerebellar mossy fiber bouton (cMFB) to granule cell (GC) synapse is an ideal model to analyze high-frequency signaling. The mechanisms underlying high-frequency transmission are discussed and compared with other synapses (Figures 3 and 4; Box 1). Finally, the function of high-frequency information coding *in vivo* at the cMFB-GC synapse are discussed (Figure 5). Note that this argumentation does not conflict with the fact that information processing occurs on a variety of time scales and that many neurons of the CNS are optimized for efficient processing of slow signals.

The role of firing frequency for neuronal information processing

In principle, a single neuron can encode information as the average firing rate (referred to as **rate coding** (see Glossary)) and/or as the exact timing of spikes in a pulse train (i.e. the temporal sequence, referred to as **temporal coding**). On the level of a population of neurons, information may be encoded using rate code (that is,

53 average asynchronous firing rate across all neurons) or temporal code, but also via a
54 correlation code, rank-order code, and/or spatiotemporal pattern code (reviewed by
55 refs. [3, 4]). It is well established that sensory information as well as motor
56 commands are predominantly encoded via rate coding. In the CNS, as sensory
57 information is processed at successive stages, average firing frequencies tend to
58 decrease and temporal- and sparse coding become increasingly important [5] (Figure
59 1A). There is a debate as to which of these coding regimes dominates in the cerebral
60 cortex, which is beyond the scope of this article (but see, e.g., refs. [5, 6]).
61 Nevertheless, rate coding is an important possibility to encode information by
62 neurons. The temporal precision of a neuronal population employing rate coding is
63 determined by both the number of neurons and the maximal firing frequency of each
64 neuron [4]. Evolutionary constraints likely define the optimal firing frequency of
65 neurons; we argue that several such constraints favor the use of fewer neurons with
66 higher firing frequency. To illustrate this, let us look at a simple example of a
67 neuronal population consisting of two neurons each with 10 Hz average firing
68 frequency (Figure 1B). Alternatively, four neurons with 5 Hz firing frequency (left) or a
69 single neuron with 20 Hz firing frequency (right) will result in the same AP frequency
70 of the ensemble (20 Hz). What are the advantages and disadvantages of these
71 scenarios?
72
73 *Advantages of higher firing frequency and fewer neurons*
74 A smaller number of high-frequency firing neurons has the advantage of ultimately
75 leading to a smaller CNS with shorter conduction delays. In addition, the CNS will
76 have a lower weight, requiring less energy to carry it. Finally, less energy is required
77 to maintain cell biological function of the smaller number of neurons (energetic costs
78 for house-keeping and resting membrane potential of each neuron; ref. [7]).

However, high-frequency firing also has the following disadvantages: In general, the metabolic efficiency of APs [8] seems to decrease with increasing firing frequency [9, 10]. Yet, APs at cMFBs, which can fire at >1 kHz frequency, are surprisingly efficient (Na^+ excess ratio of only 1.8; ref. [11]). This is currently not well understood, but argues against a biophysical requirement that metabolic efficiency decreases strongly with increasing firing frequency. Another potential disadvantage of high firing frequencies lies in the limited frequency response of synapses, which leads to a low-pass filtering of neuronal signals. Yet, some synapses can transmit exceptionally high-frequency signals (see below).

Thus, while there are strong evolutionary constraints arguing for a small number of neurons, each operating at high firing frequency, the disadvantages of high-frequency signaling are less obvious. Furthermore, some synapses, such as the cMFB-GC synapse, seem to have largely reduced these disadvantages. It should be noted, however, that less robust signaling with weak synaptic connections and recurrent excitation might benefit from a large number of neurons with low firing frequency as has been described in the cerebral cortex [6]. The major advantages of fewer, high-frequency neurons are the reduced brain size and lower basal energy consumption [7]. Energetic constraints thus argue for the use of high-frequency AP firing and synaptic transmission. Note, that the maximum firing frequency of neurons (1–2 kHz) is still more than six orders of magnitude slower compared with the clock rate of modern computers [12]. The immense effort to further increase the clock rate of computers is consistent with our argumentation. Taking into account the complex interplay of proteins required for AP generation and synaptic transmission, biophysical and energetic constraints might restrict the maximum signaling frequency of neurons. Indeed, it has previously been argued that the brain's information

processing rate may be limited to a millisecond timescale by its energy supply [13]. In summary, several arguments indicate advantages of neuronal high-frequency firing. But to what extent does high-frequency signaling occur in the CNS?

Occurrence of high-frequency signaling in the mammalian CNS

Indeed, high-frequency firing occurs ubiquitously throughout the mammalian CNS. In the cerebral cortex, subtypes of pyramidal neurons in layers 2/3 or layer 5 show a typical burst firing behavior. Within such bursts, the frequency of APs can reach up to 300 Hz. So-called *fast rhythmic bursting* or *chattering* cells may even display intraburst frequencies of ~800 Hz *in vivo* (ref. [14]; Figure 2A). Pyramidal neurons have, however, a low average firing rate of just a few Hz. A subtype of GABAergic interneurons in the cortex—fast-spiking parvalbumin-positive cells—provide feedforward inhibition as well as feedback inhibition to principal cells and are, e.g., required for network oscillations [15]. These fast-spiking interneurons can sustain AP firing at up to 500 Hz (ref. [16]; Figure 2B). Even higher AP frequencies have been observed in axons and neurons along sensory pathways. In the auditory brainstem, the localization of a sound source is achieved by processing of converging inputs from both cochleae with microsecond precision [17]. This information is first transmitted onto postsynaptic cells via large synaptic terminals, the calyces of Held. In these presynaptic terminals, spiking and synaptic transmission at up to ~1 kHz could be observed (ref. [18, 19]; Figure 2C). Also in the auditory pathway, neurons in the medial superior olive and the ventral cochlear nucleus are capable of firing APs at up to 1 kHz [20, 21]. Finally, cerebellar mossy fiber boutons (cMFBs), which convey sensory information of different origin to the cerebellar cortex, exhibit remarkably high AP frequencies. *In vivo*, AP frequencies of several hundreds of Hz were measured upon sensory stimulation, reaching instantaneous frequencies of up

to 1 kHz and average frequencies of ~350 Hz during short bursts [22, 23]. *In vitro*, APs can be reliably elicited at up to 1.6 kHz (ref. [11]; Figure 2D). To our knowledge, these AP frequencies represent the highest values in neurons reported thus far. However, it should be noted that the average firing frequencies of these example neurons are generally much slower than the here reported maximum firing frequencies.

All the above examples were collected in rodent models, but high-frequency neuronal signaling is not limited to rodents. Indeed, there are indications for high-frequency signaling in non-human primates, where high-frequency responses of ~600 Hz were observed in response to stimulation of cerebellar output neurons using functional magnetic resonance imaging [24]. In the human brain, oscillations of up to at least 600 Hz can be resolved in EEG recordings [25]. Furthermore, high-frequency signaling occurs across numerous healthy and pathological brain states. For example, it has been shown that high-frequency firing of thalamic neurons (up to 450 Hz) controls sleep [26] and that firing in the gamma-frequency (i.e., 25–100 Hz) may play a role in some neuropsychiatric diseases [27]. On the other hand, high-frequency firing has also been observed in invertebrates. Sensory touch detector cells of spiders, for instance, can fire at 600 Hz upon mechanical stimulation [28]. These examples indicate that AP firing and synaptic transmission at high frequency are fundamental for the function of the CNS in humans and throughout the animal kingdom, making the understanding of high-frequency transmission an important goal in neuroscience. In the following, we argue that the cMFB-GC synapse in rodents is an ideal model to study the mechanisms and role of high-frequency transmission in the CNS.

The cMFB-GC synapse as a model for high-frequency transmission

Structure of the cMFB-GC synapse

Mossy fibers are myelinated axons originating from cells in, e.g., spinal cord, pontine nuclei, vestibular nuclei, or cerebellar nuclei. They send collaterals to the deep cerebellar nuclei [29] and enter the GC layer of the cerebellar cortex [30], where they form several varicosities. These cMFBs have a complex shape with high surface-to-volume ratio and a relatively large diameter of 3–12 µm [31]. Ultrastructural analyses revealed that cMFBs contain a very large number of synaptic vesicles (~200,000; ref. [31]) and many **active zones** (150–300; Table I in Box 1; refs. [32, 33]).

In the **cerebellar glomeruli**, a single cMFB makes *en passant* excitatory synaptic contact with the dendrites of several cerebellar GCs. GCs have a small soma with 5–7 µm diameter and on average only four short dendrites [34-36]. The dendrites rarely exceed 20 µm in length and have a very thin diameter of ~0.6 µm [34-36]. Each GC dendrite ends in claw-shaped digits surrounding a single cMFB [37]. Estimates of the number of postsynaptic GCs per cMFB are in the range of 10–100 [11, 38], reflecting a high degree of synaptic divergence. Thus, the cMFB-GC synapse is a highly divergent synapse, structurally specialized to transmit information to many postsynaptic neurons.

Techniques for examining the cMFB-GC synapse

Patch-clamp recordings from the postsynaptic cerebellar GCs of mice *in situ* were already performed in the early 1990s [34, 39], demonstrating that low-noise and high-resolution synaptic currents could be resolved. Recently, whole-cell patch-clamp

recordings from dendrites of GCs were reported [35], which support the previously estimated electrical compactness of GCs [34, 39].

Extracellular focal recordings from presynaptic cMFBs in mice allowed measurement of changes in presynaptic currents during long-term potentiation [40]. Recently, direct presynaptic patch-clamp recordings from cMFBs in rats [22], turtles [41], and mice [11, 42-44] have extended the experimental possibilities at this synapse. Presynaptic recordings from cMFBs offer excellent voltage-clamp conditions and can be paired with recordings from postsynaptic GCs [11, 42]. Such recordings are also possible in mature animals.

Furthermore, cMFBs offer the chance to perform direct presynaptic patch-clamp recordings in anaesthetized [22] or behaving mammals (ref. [45]; cf. Table I). In addition, GCs can be recorded from *in vivo* [45, 46]. The opportunity to combine high-resolution biophysical techniques *in vitro* with direct recordings *in vivo* from both pre- and postsynaptic compartments thus makes the cMFB-GC synapse ideally suited to study neuronal high-frequency signaling.

Presynaptic mechanisms enabling high-frequency synaptic transmission

Using the above described high-resolution techniques, reliable synaptic transmission at a frequency of 1 kHz has been described at the cMFB-GC synapse (ref. [11], Figure 4A). In the following, we will review the specializations that seem essential for synaptic information transmission at such high rates and compare these mechanisms with other synapses that operate at high and low frequencies (Table I). We will

restrict our discussion on excitatory transmission (for inhibitory synapses see, e.g., refs. [47-50]) and focus on 11 points, which are illustrated in Figure 3.

(1) Short duration of the presynaptic AP

The presynaptic APs in cMFBs have a duration at half-maximal amplitude of ~100 µs (ref. [11], Figure 4C). To our knowledge, this duration is the shortest reported thus far, but such rapid APs are probably not a unique feature of cMFBs within the mammalian CNS (see Table I). However, AP duration inversely correlates with maximum firing frequency within a population of neurons (e.g. in cMFBs [11] and in neurons of the vestibular nucleus [51]), and across types of neurons [52].

(2) Fast kinetics of presynaptic ion channels

The Na^+ and K^+ currents underlying the AP have short half-durations of 73 µs and 61 µs, respectively (Figure 4C), and provide a surprising metabolic efficiency of the AP (see Table I). The AP-evoked K^+ current is mediated by voltage-gated K^+ channels of the K_V1 and K_V3 subtypes [11]. Compared with other presynaptic terminals, the contribution of the slower gating K_v1 channels [53] to the repolarization of the rapid APs at cMFBs is surprising. It is currently also unclear if the K^+ currents at cMFBs show activity-dependent facilitation to support high-frequency firing as described at the calyx of Held [54]. Despite the brevity of the APs at cMFBs, presynaptic Ca^{2+} channels—predominantly of the $Ca_v2.1$ subtype—are effectively opened during an AP [11].

(3) Low capacity of endogenous Ca^{2+} buffering

In general, Ca^{2+} ions entering a presynaptic terminal during an AP are rapidly bound by **endogenous Ca^{2+} buffers**. The binding capacity of fixed Ca^{2+} buffers at cMFBs is

very low (~15), leading to a rapid clearance of Ca^{2+} from the active zone (Figure 4C), which explains the very synchronous release of synaptic vesicles [43]. The Ca^{2+} binding capacity of endogenous buffers is similar at hippocampal mossy fiber boutons and the calyx of Held (~20 and ~45, respectively; refs. [55, 56]), but higher (~140) in boutons of cortical pyramidal neurons [57] (cf. Table I). In addition, a mobile Ca^{2+} buffer with kinetics similar to EGTA supports high-frequency firing in cMFBs by reducing the build-up of Ca^{2+} in between consecutive APs [43]. The properties of the mobile buffer at cMFBs are comparable to that at the calyx of Held synapse [58].

(4) Tight Ca^{2+} channel to vesicle coupling

The coupling distance between synaptic vesicles and Ca^{2+} channels [59, 60] is estimated to be ~20 nm at the cMFB-GC synapse (ref. [43], Figure 3). This tight **nanodomain** coupling supports a very rapid time course of release [61]. A similar coupling distance was estimated for the calyx of Held synapse [62, 63] and at parallel fiber to Purkinje cell synapses [64] (see also refs. in [60]). In contrast, hippocampal mossy fiber boutons, which operate at lower firing frequencies, exhibit a looser coupling in the range of 75 nm [65]. And the coupling distance is even larger in boutons of cortical or hippocampal pyramidal neurons (refs. [66, 67], Table I).

(5) A large pool of synaptic vesicles with fast recruitment

Initial recordings from GCs indicated that the readily releasable pool (**RRP**) for a cMFB-GC connection consists of 5–10 vesicles, and that each vesicle in the RRP is replenished from a pool of ~300 releasable vesicles with a high rate constant of 60–80 s^{-1} (refs. [68-70], Table I). Direct presynaptic depolarizations of cMFBs revealed a slightly larger RRP consisting of two populations of vesicles (~10 vesicles each) with a slightly lower rate constant of vesicle recruitment (30 s^{-1}; ref. [11]). Consistent with

these findings, a fast and slow releasing pool of vesicles has been measured at the calyx of Held synapse using presynaptic depolarization (FRP and SRP, respectively, ref. [71]), and AP-evoked release is mainly mediated by the FRP at this synapse [72]. In Table I of Box 1 we therefore differentiate between **RRP_{AP}** (corresponding to the FRP at the calyx) and **RRP_{Depol}** (corresponding to FRP+SRP at the calyx). Note, that the two pools of vesicles previously described at cMFBs [69] using AP-stimulation (i.e. within RRP_{AP}) might correspond to different degrees of **superpriming** of FRP vesicles at the calyx [73]. Finally, the high rate constant of vesicle replenishment is consistent with recent experimentally constrained modeling results on rapid diffusion of vesicles within cMFBs [74].

(6) Very rapid endocytosis

Following fusion of synaptic vesicles, the added presynaptic plasma membrane is retrieved via endocytosis. There is a considerable controversy on the speed of this process [75] and there are indications for different recycling mechanisms for membranes and vesicle proteins [151]. Endocytosis is very fast (time constant <1 s) in cultured neurons at physiological temperature [76] and room temperature [77], as well as in salamander cone photoreceptors at room temperature [78]. At the calyx of Held synapse, very fast endocytosis was observed at room temperature using membrane capacitance measurements, too [79]. But it is unclear how much this finding was influenced by artifacts [80]. The cMFB allows time-resolved high-resolution capacitance measurements at 37 °C, which revealed a rapid time constant of endocytosis following a single AP stimulus (~500 ms; ref. [42]; Figure 4B).

Postsynaptic mechanisms enabling high-frequency synaptic transmission

In addition to the presynaptic mechanisms above, sustained high-frequency transmission at the cMFB-GC synapse is supported by several specializations of the postsynaptic GCs.

(7) Rapid excitatory postsynaptic currents

The excitatory postsynaptic currents (EPSCs) recorded from GCs have very rapid rise and decay kinetics (ref. [34]; Figure 4C). GC EPSCs are predominantly mediated by AMPA receptors composed of GluA2 and GluA4 subunits [37], similar to the calyx of Held synapse [81]. In neocortical pyramidal neurons, on the other hand, GluA1 is the dominant subunit, leading to slower kinetics of AMPA mediated currents [81]. In addition, there is a contribution of NMDA receptors at the cMFB-GC synapse [34, 39], which supports synaptic transmission at high frequencies in mature synapses [82, 83].

(8) Fast recovery from glutamate receptor desensitization

The glutamate receptors in GCs enter slowly into desensitization states and have a fast recovery from desensitization [84]. This relative resistance to AMPA receptor desensitization supports high-frequency transmission, during which glutamate accumulates in the synaptic cleft.

(9) Glutamate spillover from neighboring release sites

Furthermore, there is a slow-rising component of AMPA-mediated EPSCs at the cMFB-GC synapse caused by glutamate spillover from neighboring active zones (ref. [85]; Figure 3). Spillover also contributes to the tonic component of the EPSC during frequency-dependent short-term depression [68]. This tonic component generates a

persistent depolarization mediated by both AMPA and NMDA receptors, which helps to maintain a high firing rate of GCs [22, 45].

(10) Compact synaptic ultrastructure

The cMFB-GC synapse has a compact ultrastructure with several small synaptic contacts to each GC dendrite (Table I). During development, the complexity of the glomerular structure increases [37, 86]. An increasing complexity has also been observed at the calyx of Held synapse, where more finger-like extensions occur during development [87].

(11) Electrotonic compactness of dendrites and soma

The small soma size and short dendrite length make GCs electrotonically highly compact with soma and dendrites behaving as a single electrical compartment [34, 88]. Consequently, excitatory postsynaptic potentials (EPSPs) are subject to very little dendritic filtering [35]. The compact electrotonic properties of GCs thus allow for highly efficient integration of synaptic input [89]. Interestingly, postsynaptic neurons of the calyx of Held synapse are also very compact, which differs from other synapses, where dendrites low-pass filter synaptic input (but see ref [90]).

Together, these pre- and postsynaptic specializations mediate the exceptionally rapid and high-frequency synaptic transmission with high fidelity at the cMFB-GC synapse. Several of these mechanistic findings are likely specific to high-frequent synapses, whereas other synaptic parameters are similar across different synapses operating at low- and high-frequency (see Box 1).

High-frequency coding at the cMFB-GC synapse *in vivo*

What are the functional implications of the rapid and high-frequency synaptic signaling that can take place at the cMFB-GC synapse? Earlier work using extracellular recordings in monkeys or cats indicated that mossy fiber axons exploit high-frequency rate coding of sensory variables, such as proprioceptive coding of a joint angle or eye saccade metrics, with continuous firing rates reaching 100 Hz (ref. [91, 92], Figure 5A). More recent *in vivo* recordings from GCs of anaesthetized mice demonstrated that mossy fibers carrying vestibular information, such as rotational velocity, use continuous rate coding, exhibiting a highly linear relationship between velocity and charge transfer (ref. [93], Figure 5B). In contrast, mossy fibers conveying rapid discrete sensory events, such as the sensory response to air puff stimulation, show burst firing behavior with maximum instantaneous frequencies of about 1 kHz (refs. [22, 23]; cf. Figure 2D), arguing for temporal coding. Furthermore, direct *in vivo* patch-clamp recordings from cMFBs of awake mice during locomotion indicate that some mossy fibers can shift from sparse activity to a dense rate code during movement (ref. [45], Figure 5C). How this information is transmitted to GCs has also been addressed by *in vivo* studies. GCs have a low spontaneous firing frequency of 0.5 Hz [46], but fire bursts of APs upon sensory stimulation with frequencies rarely exceeding 500 Hz [22, 45, 46]. Thus, both mossy fibers and GCs exhibit high-frequency firing *in vivo*, in particular during short bursts of activity.

The possibility of direct pre- and postsynaptic recordings *in vivo* makes the cMFB-GC an ideal model to investigate the functional role of high-frequency coding. But the exact coding at the cMFB-GC synapse is still poorly understood. Yet, from a network perspective it is clear that the main function of the cMFB-GC synapse is to distribute sensory and efferent copy information to GCs. The population of GCs is thought to detect patterns in the mossy fiber input [94], resulting in a sparser higher dimensional

code in GCs compared with mossy fibers [38]. During this information transmission, the temporal precision of the cMFB-GC synapse is essential to reliably detect rapid signals within a certain time window [95], to adaptively filter [96, 97], and to precisely match motor copy and sensory information [98]. In addition, the sequential firing of nearby GCs [99] and the successive activation of different sets of GCs [100] might underlie temporal processing in the cerebellar cortex [101]. Consistent with the role of the cerebellum in timing [100, 101], not only the frequency but also the time of AP firing in cMFBs and GCs seems essential. Independent of the diverse and partly controversial function of the cerebellar cortex, the cMFB-GC synapse thus conveys signals with remarkable bandwidth to the large number of GCs most likely using rate and temporal coding.

Concluding Remarks and Future Perspectives

Neuronal high-frequency signaling is abundant throughout the mammalian CNS (Figure 2). At the mature cMFB-GC synapse, direct pre- and postsynaptic patch-clamp recordings are feasible with excellent temporal resolution. Based on such recordings, the fastest signaling in the mammalian CNS has been described at the this synapse. Several mechanistic specializations of the cMFB-GC synapse enable precise and rapid synaptic transfer of information at very high rates (Figure 4 and Box 1). These include ultrafast APs, low endogenous calcium buffering, coupling of vesicles to calcium channels in the 20 nm range, rapid vesicle recruitment from a large pool of releasable vesicles, ultrafast endocytosis, and rapid glutamate receptors with fast recovery from desensitization. Furthermore, this synapse allows *in vivo* recordings from pre- and postsynaptic neurons, which have revealed high-frequency coding in both cMFBs and GCs (Figure 5). Thus, the cMFB-GC synapse has been

established as an attractive model to study high-frequency signaling and its implications for neuronal information processing.

More research is required to improve our understanding of high-frequency synaptic transmission (see Outstanding Questions). In this context, the use of, e.g., super-resolution microscopy [102, 103] will allow investigation of the structural-functional relationship of high-frequency synapses. To gain more insights into the molecular mechanisms, techniques allowing genetic perturbations might be extended [30]. Finally, presynaptic recordings in behaving mice [45] offer the chance to further analyze high-frequency coding during behavior.

Acknowledgements

We would like to thank Jens Eilers, Maarten H.P. Kole, Erwin Neher, and Laurens Witter for helpful discussions and comments on a previous version of the manuscript. S.H. received funding from the German Research Foundation (HA 6386/2-2 and 3-2).

References

1. Bale, M.R., *et al.* (2015) Microsecond-scale timing precision in rodent trigeminal primary afferents. *J. Neurosci.* 35, 5935–5940
2. Wagner, H., *et al.* (2005) Microsecond precision of phase delay in the auditory system of the barn owl. *J. Neurophysiol.* 94, 1655–1658
3. Kumar, A., *et al.* (2010) Spiking activity propagation in neuronal networks: reconciling different perspectives on neural coding. *Nat. Rev. Neurosci.* 11, 615–627
4. Rieke, F., *et al.* (1997) *Spikes: Exploring the Neural Code*. The MIT Press
5. Wolfe, J., *et al.* (2010) Sparse and powerful cortical spikes. *Curr. Opin. Neurobiol.* 20, 306–312
6. Tchumatchenko, T., *et al.* (2011) Ultrafast population encoding by cortical neurons. *J. Neurosci.* 31, 12171–12179
7. Harris, J.J. and Attwell, D. (2012) The energetics of CNS white matter. *J. Neurosci.* 32, 356–371
8. Alle, H., *et al.* (2009) Energy-efficient action potentials in hippocampal mossy fibers. *Science* 325, 1405–1408
9. Carter, B.C. and Bean, B.P. (2011) Incomplete inactivation and rapid recovery of voltage-dependent sodium channels during high-frequency firing in cerebellar Purkinje neurons. *J. Neurophysiol.* 105, 860–871
10. Hallermann, S., *et al.* (2012) State and location dependence of action potential metabolic cost in cortical pyramidal neurons. *Nat. Neurosci.* 15, 1007–1014
11. Ritzau-Jost, A., *et al.* (2014) Ultrafast action potentials mediate kilohertz signaling at a central synapse. *Neuron* 84, 152–163
12. Nagarajan, N. and Stevens, C.F. (2008) How does the speed of thought compare for brains and digital computers? *Curr. Biol.* 18, R756–R758
13. Attwell, D. and Gibb, A. (2005) Neuroenergetics and the kinetic design of excitatory synapses. *Nat. Rev. Neurosci.* 6, 841–849
14. Gray, C.M. and McCormick, D.A. (1996) Chattering cells: superficial pyramidal neurons contributing to the generation of synchronous oscillations in the visual cortex. *Science* 274, 109–113
15. Hu, H., *et al.* (2014) Interneurons. Fast-spiking, parvalbumin^{+} GABAergic interneurons: from cellular design to microcircuit function. *Science* 345, 1255263
16. Azouz, R., *et al.* (1997) Physiological properties of inhibitory interneurons in cat striate cortex. *Cereb. Cortex* 7, 534–545
17. Trussell, L.O. (1999) Synaptic mechanisms for coding timing in auditory neurons. *Annu. Rev. Physiol.* 61, 477–496
18. Kim, J.H., *et al.* (2013) Dysmyelination of auditory afferent axons increases the jitter of action potential timing during high-frequency firing. *J. Neurosci.* 33, 9402–9407
19. Blosa, M., *et al.* (2015) The extracellular matrix molecule brevican is an integral component of the machinery mediating fast synaptic transmission at the calyx of Held. *J. Physiol.* 593, 4341–4360
20. Scott, L.L., *et al.* (2007) Weak action potential backpropagation is associated with high-frequency axonal firing capability in principal neurons of the gerbil medial superior olive. *J. Physiol.* 583, 647–661

21. Oertel, D., *et al.* (2000) Detection of synchrony in the activity of auditory nerve fibers by octopus cells of the mammalian cochlear nucleus. *Proc. Natl. Acad. Sci. USA* 97, 11773–11779
22. Rancz, E.A., *et al.* (2007) High-fidelity transmission of sensory information by single cerebellar mossy fibre boutons. *Nature* 450, 1245–1248
23. Garwicz, M., *et al.* (1998) Cutaneous receptive fields and topography of mossy fibres and climbing fibres projecting to cat cerebellar C3 zone. *J. Physiol.* 512, 277–293
24. Sultan, F., *et al.* (2012) Unravelling cerebellar pathways with high temporal precision targeting motor and extensive sensory and parietal networks. *Nat. Commun.* 3, 924
25. Ritter, P., *et al.* (2008) High-frequency (600 Hz) population spikes in human EEG delineate thalamic and cortical fMRI activation sites. *NeuroImage* 42, 483–490
26. McCormick, D.A. and Bal, T. (1997) Sleep and arousal: thalamocortical mechanisms. *Annu. Rev. Neurosci.* 20, 185–215
27. Sauer, J.F., *et al.* (2015) Impaired fast-spiking interneuron function in a genetic mouse model of depression. *eLife* 4, e04979
28. Albert, J.T., *et al.* (2001) Arthropod touch reception: spider hair sensilla as rapid touch detectors. *J. Comp. Physiol. A* 187, 303–312
29. Pugh, J.R. and Raman, I.M. (2006) Potentiation of mossy fiber EPSCs in the cerebellar nuclei by NMDA receptor activation followed by postinhibitory rebound current. *Neuron* 51, 113–123
30. Kalinovsky, A., *et al.* (2011) Development of axon-target specificity of ponto-cerebellar afferents. *PLoS Biol.* 9, e1001013
31. Rollenhagen, A., *et al.* (2007) Structural determinants of transmission at large hippocampal mossy fiber synapses. *J. Neurosci.* 27, 10434–10444
32. Kim, H.W., *et al.* (2013) Three-dimensional imaging of cerebellar mossy fiber rosettes by ion-abrasion scanning electron microscopy. *Microsc. Microanal.* 19 Suppl 5, 172–177
33. Xu-Friedman, M.A. and Regehr, W.G. (2003) Ultrastructural contributions to desensitization at cerebellar mossy fiber to granule cell synapses. *J. Neurosci.* 23, 2182–2192
34. Silver, R.A., *et al.* (1992) Rapid-time-course miniature and evoked excitatory currents at cerebellar synapses in situ. *Nature* 355, 163–166
35. Delvendahl, I., *et al.* (2015) Dendritic patch-clamp recordings from cerebellar granule cells demonstrate electrotonic compactness. *Front. Cell. Neurosci.* 9, 93
36. Cathala, L., *et al.* (2003) Maturation of EPSCs and intrinsic membrane properties enhances precision at a cerebellar synapse. *J. Neurosci.* 23, 6074–6085
37. Cathala, L., *et al.* (2005) Changes in synaptic structure underlie the developmental speeding of AMPA receptor-mediated EPSCs. *Nat. Neurosci.* 8, 1310–1318
38. Billings, G., *et al.* (2014) Network structure within the cerebellar input layer enables lossless sparse encoding. *Neuron* 83, 960–974
39. D'Angelo, E., *et al.* (1990) Dual-component NMDA receptor currents at a single central synapse. *Nature* 346, 467–470
40. Maffei, A., *et al.* (2002) Presynaptic current changes at the mossy fiber-granule cell synapse of cerebellum during LTP. *J. Neurophysiol.* 88, 627–638

41. Thomsen, L.B., *et al.* (2010) Presynaptic calcium signalling in cerebellar mossy fibres. *Front. Neural Circuits* 4, 1
42. Delvendahl, I., *et al.* (2016) Fast, Temperature-Sensitive and Clathrin-Independent Endocytosis at Central Synapses. *Neuron* 90, 492–498
43. Delvendahl, I., *et al.* (2015) Reduced endogenous Ca^{2+} buffering speeds active zone Ca^{2+} signaling. *Proc. Natl. Acad. Sci. USA* 112, E3075–3084
44. Gao, Z., *et al.* (2016) Excitatory Cerebellar Nucleocortical Circuit Provides Internal Amplification during Associative Conditioning. *Neuron* 89, 645–657
45. Powell, K., *et al.* (2015) Synaptic representation of locomotion in single cerebellar granule cells. *eLife* 4, e07290
46. Chadderton, P., *et al.* (2004) Integration of quanta in cerebellar granule cells during sensory processing. *Nature* 428, 856–860
47. Rowan, M.J., *et al.* (2016) Synapse-Level Determination of Action Potential Duration by K^+ Channel Clustering in Axons. *Neuron* 91, 370–383
48. Kawaguchi, S.Y. and Sakaba, T. (2015) Control of inhibitory synaptic outputs by low excitability of axon terminals revealed by direct recording. *Neuron* 85, 1273–1288
49. Begum, R., *et al.* (2016) Action potential broadening in a presynaptic channelopathy. *Nat. Commun.* 7, 12102
50. Hu, H. and Jonas, P. (2014) A supercritical density of Na^+ channels ensures fast signaling in GABAergic interneuron axons. *Nat. Neurosci.* 17, 686–693
51. Gittis, A.H., *et al.* (2010) Mechanisms of sustained high firing rates in two classes of vestibular nucleus neurons: differential contributions of resurgent Na, Kv3, and BK currents. *J. Neurophysiol.* 104, 1625–1634
52. Carter, B.C. and Bean, B.P. (2009) Sodium entry during action potentials of mammalian neurons: incomplete inactivation and reduced metabolic efficiency in fast-spiking neurons. *Neuron* 64, 898–909
53. Alle, H., *et al.* (2011) Sparse but highly efficient Kv3 outpace BKCa channels in action potential repolarization at hippocampal mossy fiber boutons. *J. Neurosci.* 31, 8001–8012
54. Yang, Y.M., *et al.* (2014) Enhancing the fidelity of neurotransmission by activity-dependent facilitation of presynaptic potassium currents. *Nat. Commun.* 5, 4564
55. Helmchen, F., *et al.* (1997) Calcium dynamics associated with a single action potential in a CNS presynaptic terminal. *Biophys. J.* 72, 1458–1471
56. Jackson, M.B. and Redman, S.J. (2003) Calcium dynamics, buffering, and buffer saturation in the boutons of dentate granule-cell axons in the hilus. *J. Neurosci.* 23, 1612–1621
57. Koester, H.J. and Sakmann, B. (2000) Calcium dynamics associated with action potentials in single nerve terminals of pyramidal cells in layer 2/3 of the young rat neocortex. *J. Physiol.* 529, 625–646
58. Müller, M., *et al.* (2007) Parvalbumin is a mobile presynaptic Ca^{2+} buffer in the calyx of held that accelerates the decay of Ca^{2+} and short-term facilitation. *J. Neurosci.* 27, 2261–2271
59. Eggermann, E., *et al.* (2012) Nanodomain coupling between Ca^{2+} channels and sensors of exocytosis at fast mammalian synapses. *Nat. Rev. Neurosci.* 13, 7–21
60. Stanley, E.F. (2016) The nanophysiology of fast transmitter release. *Trends Neurosci.* 39, 183–197

61. Sargent, P.B., *et al.* (2005) Rapid vesicular release, quantal variability, and spillover contribute to the precision and reliability of transmission at a glomerular synapse. *J. Neurosci.* 25, 8173–8187
62. Wang, L.Y., *et al.* (2008) Synaptic vesicles in mature calyx of Held synapses sense higher nanodomain calcium concentrations during action potential-evoked glutamate release. *J. Neurosci.* 28, 14450–14458
63. Nakamura, Y., *et al.* (2015) Nanoscale Distribution of Presynaptic Ca^{2+} Channels and Its Impact on Vesicular Release during Development. *Neuron* 85, 145–158
64. Schmidt, H., *et al.* (2013) Nanodomain Coupling at an Excitatory Cortical Synapse. *Curr. Biol.* 23, 244–249
65. Vyleta, N.P. and Jonas, P. (2014) Loose coupling between Ca^{2+} channels and release sensors at a plastic hippocampal synapse. *Science* 343, 665–670
66. Rozov, A., *et al.* (2001) Transmitter release modulation by intracellular Ca^{2+} buffers in facilitating and depressing nerve terminals of pyramidal cells in layer 2/3 of the rat neocortex indicates a target cell-specific difference in presynaptic calcium dynamics. *J. Physiol.* 531, 807–826
67. Ohana, O. and Sakmann, B. (1998) Transmitter release modulation in nerve terminals of rat neocortical pyramidal cells by intracellular calcium buffers. *J. Physiol.* 513, 135–148
68. Saviane, C. and Silver, R.A. (2006) Fast vesicle reloading and a large pool sustain high bandwidth transmission at a central synapse. *Nature* 439, 983–987
69. Hallermann, S., *et al.* (2010) Bassoon speeds vesicle reloading at a central excitatory synapse. *Neuron* 68, 710–723
70. Hallermann, S. and Silver, R.A. (2013) Sustaining rapid vesicular release at active zones: potential roles for vesicle tethering. *Trends Neurosci.* 36, 185–194
71. Neher, E. and Sakaba, T. (2008) Multiple roles of calcium ions in the regulation of neurotransmitter release. *Neuron* 59, 861–872
72. Sakaba, T. (2006) Roles of the fast-releasing and the slowly releasing vesicles in synaptic transmission at the calyx of Held. *J. Neurosci.* 26, 5863–5871
73. Taschenberger, H., *et al.* (2016) Superpriming of synaptic vesicles as a common basis for intersynapse variability and modulation of synaptic strength. *Proc. Natl. Acad. Sci. USA* 113, E4548–4557
74. Rothman, J.S., *et al.* (2016) Physical determinants of vesicle mobility and supply at a central synapse. *eLife* 5, in press (doi: 10.7554/eLife.15133)
75. Kononenko, N.L. and Haucke, V. (2015) Molecular mechanisms of presynaptic membrane retrieval and synaptic vesicle reformation. *Neuron* 85, 484–496
76. Watanabe, S., *et al.* (2013) Ultrafast endocytosis at mouse hippocampal synapses. *Nature* 504, 242–247
77. Leitz, J. and Kavalali, E.T. (2014) Fast retrieval and autonomous regulation of single spontaneously recycling synaptic vesicles. *eLife* 3, e03658
78. Van Hook, M.J. and Thoreson, W.B. (2012) Rapid synaptic vesicle endocytosis in cone photoreceptors of salamander retina. *J. Neurosci.* 32, 18112–18123
79. Sun, J.Y., *et al.* (2002) Single and multiple vesicle fusion induce different rates of endocytosis at a central synapse. *Nature* 417, 555–559
80. Yamashita, T., *et al.* (2005) Vesicle endocytosis requires dynamin-dependent GTP hydrolysis at a fast CNS synapse. *Science* 307, 124–127

81. Geiger, J.R., *et al.* (1995) Relative abundance of subunit mRNAs determines gating and Ca2+ permeability of AMPA receptors in principal neurons and interneurons in rat CNS. *Neuron* 15, 193–204
82. D'Angelo, E., *et al.* (1995) Synaptic excitation of individual rat cerebellar granule cells in situ: evidence for the role of NMDA receptors. *J. Physiol.* 484, 397–413
83. Baade, C., *et al.* (2016) NMDA receptors amplify mossy fiber synaptic inputs at frequencies up to at least 750 Hz in cerebellar granule cells. *Synapse* 70, 269–276
84. DiGregorio, D.A., *et al.* (2007) Desensitization properties of AMPA receptors at the cerebellar mossy fiber granule cell synapse. *J. Neurosci.* 27, 8344–8357
85. DiGregorio, D.A., *et al.* (2002) Spillover of glutamate onto synaptic AMPA receptors enhances fast transmission at a cerebellar synapse. *Neuron* 35, 521–533
86. Hámori, J. and Somogyi, J. (1983) Differentiation of cerebellar mossy fiber synapses in the rat: a quantitative electron microscope study. *J. Comp. Neurol.* 220, 365–377
87. Taschenberger, H., *et al.* (2002) Optimizing synaptic architecture and efficiency for high-frequency transmission. *Neuron* 36, 1127–1143
88. D'Angelo, E., *et al.* (1993) Different proportions of N-methyl-D-aspartate and non-N-methyl-D-aspartate receptor currents at the mossy fibre-granule cell synapse of developing rat cerebellum. *Neuroscience* 53, 121–130
89. London, M. and Häusser, M. (2005) Dendritic computation. *Annu. Rev. Neurosci.* 28, 503–532
90. Golding, N.L. and Oertel, D. (2012) Synaptic integration in dendrites: exceptional need for speed. *J. Physiol.* 590, 5563–5569
91. van Kan, P.L., *et al.* (1993) Movement-related inputs to intermediate cerebellum of the monkey. *J. Neurophysiol.* 69, 74–94
92. Prsa, M., *et al.* (2009) Characteristics of responses of Golgi cells and mossy fibers to eye saccades and saccadic adaptation recorded from the posterior vermis of the cerebellum. *J. Neurosci.* 29, 250–262
93. Arenz, A., *et al.* (2008) The contribution of single synapses to sensory representation in vivo. *Science* 321, 977–980
94. Marr, D. (1969) A theory of cerebellar cortex. *J. Physiol.* 202, 437–470
95. D'Angelo, E. and De Zeeuw, C.I. (2009) Timing and plasticity in the cerebellum: focus on the granular layer. *Trends Neurosci.* 32, 30–40
96. Jörntell, H. and Ekerot, C.F. (2006) Properties of somatosensory synaptic integration in cerebellar granule cells in vivo. *J. Neurosci.* 26, 11786–11797
97. Dean, P., *et al.* (2010) The cerebellar microcircuit as an adaptive filter: experimental and computational evidence. *Nat. Rev. Neurosci.* 11, 30–43
98. Kennedy, A., *et al.* (2014) A temporal basis for predicting the sensory consequences of motor commands in an electric fish. *Nat. Neurosci.* 17, 416–422
99. Heck, D., *et al.* (2001) Sequential stimulation of rat cerebellar granular layer in vivo: Further evidence of a 'tidal-wave' timing mechanism in the cerebellum. *Neurocomputing* 38, 641–646
100. Medina, J.F., *et al.* (2000) Timing mechanisms in the cerebellum: testing predictions of a large-scale computer simulation. *J. Neurosci.* 20, 5516–5525
101. Mauk, M.D. and Buonomano, D.V. (2004) The neural basis of temporal processing. *Annu. Rev. Neurosci.* 27, 307–340

652 102. Ehmann, N.*, et al.* (2014) Quantitative super-resolution imaging of Bruchpilot
653 distinguishes active zone states. *Nat. Commun.* 5, 4650
654 103. Nanguneri, S.*, et al.* (2012) Three-dimensional, tomographic super-resolution
655 fluorescence imaging of serially sectioned thick samples. *PloS one* 7, e38098
656 104. Wang, S.S.*, et al.* (2016) Fusion Competent Synaptic Vesicles Persist upon
657 Active Zone Disruption and Loss of Vesicle Docking. *Neuron* 91, 777-791
658 105. Neher, E. (2015) Merits and Limitations of Vesicle Pool Models in View of
659 Heterogeneous Populations of Synaptic Vesicles. *Neuron* 87, 1131-1142
660 106. Thanawala, M.S. and Regehr, W.G. (2013) Presynaptic calcium influx controls
661 neurotransmitter release in part by regulating the effective size of the readily
662 releasable pool. *J. Neurosci.* 33, 4625-4633
663 107. Pan, B. and Zucker, R.S. (2009) A general model of synaptic transmission and
664 short-term plasticity. *Neuron* 62, 539-554
665 108. Kole, M.H. (2011) First node of Ranvier facilitates high-frequency burst
666 encoding. *Neuron* 71, 671–682
667 109. de Kock, C.P. and Sakmann, B. (2008) High frequency action potential bursts
668 (>or= 100 Hz) in L2/3 and L5B thick tufted neurons in anaesthetized and
669 awake rat primary somatosensory cortex. *J. Physiol.* 586, 3353–3364
670 110. Renden, R. and von Gersdorff, H. (2007) Synaptic vesicle endocytosis at a
671 CNS nerve terminal: faster kinetics at physiological temperatures and
672 increased endocytotic capacity during maturation. *J. Neurophysiol.* 98, 3349–
673 3359
674 111. Molnár, G.*, et al.* (2016) Human pyramidal to interneuron synapses are
675 mediated by multi-vesicular release and multiple docked vesicles. *eLife* 5,
676 e18167
677 112. Pernia-Andrade, A.J. and Jonas, P. (2014) Theta-gamma-modulated synaptic
678 currents in hippocampal granule cells in vivo define a mechanism for network
679 oscillations. *Neuron* 81, 140–152
680 113. Lisman, J. (1997) Bursts as a unit of neural information: making unreliable
681 synapses reliable. *Trends Neurosci.* 20, 38–43
682 114. Forsythe, I.D. (1994) Direct patch recording from identified presynaptic
683 terminals mediating glutamatergic EPSCs in the rat CNS, in vitro. *J. Physiol.*
684 479, 381–387
685 115. Geiger, J.R.P. and Jonas, P. (2000) Dynamic control of presynaptic Ca^{2+}
686 inflow by fast-inactivating K^+ channels in hippocampal mossy fiber boutons.
687 *Neuron* 28, 927–939
688 116. Jakab, R.L. and Hámori, J. (1988) Quantitative morphology and synaptology
689 of cerebellar glomeruli in the rat. *Anat. Embryol.* 179, 81–88
690 117. Hoffpauir, B.K.*, et al.* (2006) Synaptogenesis of the calyx of Held: rapid onset
691 of function and one-to-one morphological innervation. *J. Neurosci.* 26, 5511–
692 5523
693 118. Koester, H.J. and Johnston, D. (2005) Target cell-dependent normalization of
694 transmitter release at neocortical synapses. *Science* 308, 863–866
695 119. Holderith, N.*, et al.* (2012) Release probability of hippocampal glutamatergic
696 terminals scales with the size of the active zone. *Nat. Neurosci.* 15, 988–997
697 120. Sätzler, K.*, et al.* (2002) Three-dimensional reconstruction of a calyx of Held
698 and its postsynaptic principal neuron in the medial nucleus of the trapezoid
699 body. *J. Neurosci.* 22, 10567–10579
700 121. Silver, R.A.*, et al.* (2003) High-probability uniquantal transmission at excitatory
701 synapses in barrel cortex. *Science* 302, 1981–1984

122. Schikorski, T. and Stevens, C.F. (1997) Quantitative ultrastructural analysis of hippocampal excitatory synapses. *J. Neurosci.* 17, 5858–5867
123. Taschenberger, H. and von Gersdorff, H. (2000) Fine-tuning an auditory synapse for speed and fidelity: developmental changes in presynaptic waveform, EPSC kinetics, and synaptic plasticity. *J. Neurosci.* 20, 9162–9173
124. Kole, M.*, et al.* (2007) Axon initial segment Kv1 channels control axonal action potential waveform and synaptic efficacy. *Neuron* 55, 633–647
125. Leão, R.M.*, et al.* (2005) Presynaptic Na^+ channels: locus, development, and recovery from inactivation at a high-fidelity synapse. *J. Neurosci.* 25, 3724–3738
126. Sola, E.*, et al.* (2004) Increased neurotransmitter release during long-term potentiation at mossy fibre-granule cell synapses in rat cerebellum. *J. Physiol.* 557, 843–861
127. Schneggenburger, R. and Neher, E. (2000) Intracellular calcium dependence of transmitter release rates at a fast central synapse. *Nature* 406, 889–893
128. Hosoi, N.*, et al.* (2007) Quantitative analysis of calcium-dependent vesicle recruitment and its functional role at the calyx of Held synapse. *J. Neurosci.* 27, 14286–14298
129. Lawrence, J.J.*, et al.* (2004) Quantal transmission at mossy fibre targets in the CA3 region of the rat hippocampus. *J. Physiol.* 554, 175–193
130. Rosenmund, C.*, et al.* (1993) Nonuniform Probability of Glutamate Release at a Hippocampal Synapse. *Science* 262, 754–757
131. Branco, T.*, et al.* (2008) Local Dendritic Activity Sets Release Probability at Hippocampal Synapses. *Neuron* 59, 475–485
132. Nadkarni, S.*, et al.* (2012) Short-term plasticity constrains spatial organization of a hippocampal presynaptic terminal. *Proc. Natl. Acad. Sci. USA* 109, 14657–14662
133. Scimemi, A. and Diamond, J.S. (2012) The number and organization of Ca^{2+} channels in the active zone shapes neurotransmitter release from schaffer collateral synapses. *J. Neurosci.* 32, 18157–18176
134. Schikorski, T. and Stevens, C.F. (2001) Morphological correlates of functionally defined synaptic vesicle populations. *Nat. Neurosci.* 4, 391–395
135. Hallermann, S.*, et al.* (2003) A large pool of releasable vesicles in a cortical glutamatergic synapse. *Proc. Natl. Acad. Sci. USA* 100, 8975–8980
136. Kushmerick, C.*, et al.* (2006) Physiological temperatures reduce the rate of vesicle pool depletion and short-term depression via an acceleration of vesicle recruitment. *J. Neurosci.* 26, 1366–1377
137. Neher, E. (2010) What is Rate-Limiting during Sustained Synaptic Activity: Vesicle Supply or the Availability of Release Sites. *Front. Synaptic Neurosci.* 2, 144
138. Klyachko, V.A. and Stevens, C.F. (2006) Temperature-dependent shift of balance among the components of short-term plasticity in hippocampal synapses. *J. Neurosci.* 26, 6945–6957
139. Lin, K.H.*, et al.* (2011) Presynaptic Ca^{2+} influx and vesicle exocytosis at the mouse endbulb of Held: a comparison of two auditory nerve terminals. *J. Physiol.* 589, 4301–4320
140. Han, Y.Y.*, et al.* (2015) RIM1 and RIM2 redundantly determine Ca^{2+} channel density and readily releasable pool size at a large hindbrain synapse. *J. Neurophysiol.* 113, 255–263
141. Bischofberger, J.*, et al.* (2002) Timing and efficacy of Ca^{2+} channel activation in hippocampal mossy fiber boutons. *J. Neurosci.* 22, 10593–10602

142. Novak, P.*, et al.* (2013) Nanoscale-targeted patch-clamp recordings of functional presynaptic ion channels. *Neuron* 79, 1067–1077
143. Müller, A.*, et al.* (2005) Endogenous Ca^{2+} buffer concentration and Ca^{2+} microdomains in hippocampal neurons. *J. Neurosci.* 25, 558–565
144. Shu, Y.*, et al.* (2006) Modulation of intracortical synaptic potentials by presynaptic somatic membrane potential. *Nature* 441, 761–765
145. Smith, S.M.*, et al.* (2004) Recordings from single neocortical nerve terminals reveal a nonselective cation channel activated by decreases in extracellular calcium. *Neuron* 41, 243–256
146. Sasaki, T.*, et al.* (2011) Action-potential modulation during axonal conduction. *Science* 331, 599–601
147. Chabrol, F.P.*, et al.* (2015) Synaptic diversity enables temporal coding of coincident multisensory inputs in single neurons. *Nat. Neurosci.* 18, 718–727
148. Guzman, S.J.*, et al.* (2016) Synaptic mechanisms of pattern completion in the hippocampal CA3 network. *Science* 353, 1117–1123
149. Keller, D.*, et al.* (2015) An Exclusion Zone for Ca^{2+} Channels around Docked Vesicles Explains Release Control by Multiple Channels at a CNS Synapse. *PLoS Comput. Biol.* 11, e1004253
150. Lee, J.S.*, et al.* (2012) Actin-dependent rapid recruitment of reluctant synaptic vesicles into a fast-releasing vesicle pool. *Proc. Natl. Acad. Sci. USA* 109, E765–774
151. Okamoto, Y., *et al.* (2016) Distinct modes of endocytotic presynaptic membrane and protein uptake at the calyx of Held terminal of rats and mice. *eLife* 5, e14643

Glossary

Active Zone: refers to the specialized area of presynaptic plasma membrane and the associated protein network where vesicle release occurs. Active zones thus include presynaptic Ca^{2+} channels and several evolutionary conserved proteins that are involved in docking and priming of synaptic vesicles, recruitment of Ca^{2+} channels, and tethering of vesicles. Note that active zones are not required for fusion competence of vesicles per se [104], but rather seem to increase release probability and organize vesicle recruitment.

Cerebellar glomerulus: contains a single mossy fiber bouton or terminal that contacts several granule cell dendrites and Golgi cell dendrites. In addition, a cerebellar glomerulus typically also includes axons of inhibitory Golgi cells. The glomerular structure is ensheathed by glia.

Deconvolution technique: can be used to estimate the time course of presynaptic vesicle release by measuring the postsynaptic current. The current is deconvolved using the measured waveform of miniature postsynaptic currents originating from spontaneous single vesicle fusion and a calculated 'residual' current due to glutamate accumulation in the synaptic cleft. For this type of deconvolution analysis, paired recordings between presynaptic terminal and postsynaptic neuron are required.

Endogenous Ca^{2+} buffers: these are proteins with Ca^{2+} binding domains that alter the spatiotemporal characteristics of intracellular Ca^{2+}. Endogenous Ca^{2+} buffers can be classified as fixed (immobile) or mobile. Typical proteins that constitute endogenous mobile buffers include calretinin, parvalbumin, and calbindin, whereas the identity of endogenous fixed Ca^{2+} buffers remains largely unknown.

Nanodomain: refers to a very localized presynaptic Ca^{2+} signal that governs release of synaptic vesicles. Nanodomain coupling usually refers to vesicle-to-Ca^{2+}-channel

804 distances of <100 nm, with larger distances being termed microdomain. The vesicle-
805 to-Ca^{2+}-channel may change during development, and many adult synapses rely on
806 nanodomain coupling.
807 **Rate coding:** can be used by neurons to represent information. For rate-coded
808 signaling, the frequency of APs within a certain time frame—and not the temporal
809 occurrence of APs—conveys the required information. Rate coding is typical in many
810 sensory systems and motoneurons.
811 **RRP:** The pool of readily releasable vesicles is heterogeneous [105, 106] and might
812 even be a “fussy concept” [107]. Here, we differentiate between the RRP that can be
813 evoked by APs (RRP_{AP}) and by depolarizations (RRP_{Depol}).
814 **RRP_{AP}:** is measured with, e.g., fluctuation analysis and back-extrapolations [105,
815 106], but postsynaptic receptor saturation can cause an underestimation of this RRP.
816 **RRP_{Depol}:** With depolarizations, an additional pool of slowly releasing vesicles (SRP;
817 ref. [71]) can be released, which is probably not being released by APs [72].
818 However, dissecting SRP and vesicle recruitment is difficult. In general, the higher
819 the rate of vesicle recruitment is assumed, the smaller the RRP will be. For example,
820 neglecting vesicle recruitment during depolarizations (with a duration of often
821 >30 ms) or sucrose application (often >1 s) can lead to an overestimation of the
822 RRP.
823 **Superpriming:** describes an additional increase in release probability of synaptic
824 vesicles after having been docked and primed at the presynaptic plasma membrane.
825 **Temporal coding:** refers to a type of information representation that relies on the
826 temporal correlation of APs in different neurons. Temporal coding can be used for
827 coincidence detection and plays an important role in oscillating neuronal networks.
828

Trends Box

- Recent studies using high-resolution methods revealed the remarkable speed of synaptic transmission at central synapses.
- Very rapid release of presynaptic vesicles is supported by fast ion channels, brief action potentials, fast vesicle recruitment, and tight nanodomain coupling.
- Fast kinetics of excitatory postsynaptic currents ensures rapid and efficient integration.
- Mechanisms of high-frequency transmission may be similar between different types of synapses.

Outstanding Questions Box

- In previous studies, the frequency of action potential firing and of synaptic transmission may have been underestimated due to limited temporal resolution (see Box 1). Are other synapses capable of similar high-frequency signaling?
- Does the ability of a synapse to operate at high-frequency indicate that such frequencies are used *in vivo*? Or in other words, did previous *in vivo* studies in anaesthetized or head fixed animals underestimate the maximal firing frequencies that could occur during, e.g., fight-and-flight reactions?
- What are the molecular mechanisms underlying high-frequency transmission? Is this synaptic feature mediated by stoichiometry of the proteins or by functional modifications of proteins such as phosphorylation?
- What are the ultrastructural specializations of synapses and active zones enabling high-frequency synaptic transmission?
- What are the important cues locally to induce the formation of cMFBs originating from various brain regions?
- How high are the metabolic costs of neuronal high-frequency signaling?

Box 1: Tuning of synapses for high-frequency signaling

To better understand how synapses are tuned for high-frequency signaling, we here compare synaptic parameters of several excitatory synapses with gradually decreasing instantaneous maximum firing frequencies *in vivo* (Table I): The cMFB-GC and the calyx of Held synapse with very high frequency, neocortical pyramidal cells with layer- and cell-type-specific intermediate frequency, and hippocampal synapses with lower frequencies.

The high connectivity (Table I) of the cMFB is a unique feature among these synapses. The number of active zones (Table I) varies among both high- and low-frequency synapses. In contrast, the AP half-width (Table I) appears to be related to maximum firing frequency. However, small errors in pipette capacitance compensation can cause under- or overestimation of AP duration (and notably also of the maximum firing frequency). The metabolic efficiency and the Ca^{2+} channel to vesicle coupling distance (Table I) also seem to be linked to firing frequency. Thus, high-frequency synapses tend to have rapid APs with rather low metabolic efficiency [8, 10, 52] and exhibit tight Ca^{2+} channel to vesicle coupling [59, 60].

Regarding the remaining parameters, there is a striking lack of reliable quantitative data. In particular, the fundamental parameter of the RRP per active zone is difficult to define and measure [105]. To facilitate comparison, we differentiate between an RRP that can be released by APs (RRP_{AP}) and an RRP that can be released by presynaptic depolarizations (RRP_{Depol}; see Glossary for more information). Despite the difficulty to accurately measure RRPs and number of AZs, cMFBs seem to have a uniquely small RRP_{AP} and RRP_{Depol} per AZ, consistent with their small active zone diameter (Table I) [70]. Furthermore, the high rate constant of vesicle replenishment and the high release probability (Table I) seem specific for cMFBs and not

characteristic for high-frequency synapses. But there is still a surprising uncertainty in the rate of vesicle recruitment, which seems related to the limited precision of the RRP definition (see above; [70]). The Ca^{2+}-binding ratio (κ_E; Table I) is often not differentiated for fixed ($\kappa_{E.fix}$) and mobile buffers, which complicates a comparison. Furthermore, estimates based on dye loading of boutons via the somatic patch pipette can cause underestimation of $\kappa_{E.fix}$. Nevertheless, with the exception of $\kappa_{E.fix}$ = 20 at the hMFB, high-frequency synapses tend to have a lower $\kappa_{E.fix}$ [43].

Thus, while there is a considerable heterogeneity of the functional parameters among high-frequency synapses (here, the cMFB-GC and the calyx of Held synapse), some parameters seem to tune synapses for high-frequency transmission. Yet, there is a surprising uncertainty in many of these fundamental parameters. In particular, the estimates often critically depend on the used technique (e.g. RRP_{AP} vs. RRP_{Depol}), recording temperature (e.g., ref. [110]), and possibly also the exact species (e.g., ref. [111]).

898 **Table I. Properties of high- and low-frequency excitatory synapses**

Property	Unit	cMFB	Calyx of Held	Boutons of neocortical pyramidal cells	Hippocampal MFB	Boutons of Schaffer collateral
Maximum instantaneous firing frequency *in vivo*	Hz	<1200 [22, 23, 92]	<800 [19]	<100 (L2/3 barrel) [109] <350 (L5B) [109] <800 (L2/3 visual) [14]	<150 [112]	<100 [113]
Presynaptic recordings established (brain slice/in vivo)		yes/yes [22, 45]	yes/no [114]	no/no [a]	yes/no [115]	no/no [b]
Connectivity per synapse		1:12–1:50 [38, 116]	1:1 [117]	1:1 [118]	1:1 [31]	1:1 [119]
No. of AZs		150–300 [32, 33, 116]	600 [120]	1 [118, 121]	25 [31]	1 [119]
Diameter of AZs	nm	~150 [74, 86]	~300 [120]	~250 [111]	~300 [120]	~200 [119, 122]
AP half-width	µs	110 [11]	~100 predicted [123]	270 [124] [c]	380 [115]	n.d.
Metabolic efficiency of AP		1.8 [11]	no Na^+ current [125]	2 [10]	1.3 [8]	n.d.
Release probability per vesicle		0.4–0.6 [68, 69, 126] [d]	0.05–0.2 [127, 128]	0.1–0.9 [118, 121]	<0.1 –0.15 [65, 129]	0.1–0.6 [119, 130, 131] [e]
Ca^{2+} channel to vesicle coupling distance	nm	~20 [43]	~20 [62, 63] [f]	n.d. [g]	~75 [65]	30–300 [132, 133]
RRP_{AP} per AZ		1 [11, 68, 69, 126] [h]	3 [71]	2–10 [111, 134]	2 [65] [i]	4 [133]
RRP_{Depol} per AZ		3 [11] [j]	3–6 [71]	n.d.	30 [135]	n.d.
Replenishment rate constant	s^{-1}	30–80 [11, 68, 69]	3–11 [136, 137] [k]	n.d.	n.d.	0.8 [138]
Exocytosis efficiency	fF pC^{-1}	65 [42]	45 [139]	n.d.	20 [42]	n.d.
Ca^{2+} current density	pA pF^{-1}	145 [42]	70 [139, 140]	n.d.	70 [141]	500 [142]
AP residual $[Ca^{2+}]$ amplitude	nM	220 [43]	500 [55]	n.d.	1,000 [56]	n.d.
AP residual $[Ca^{2+}]$ τ decay	ms	25 [43]	45 [55]	55 [57]	45 [56]	n.d.
Ca^{2+}-binding ratio (κ_E) of fixed buffer		15 [43]	45 [55]	140 [57]	20 [56]	n.d.
Ca^{2+}-binding ratio (κ_E) of mobile buffer		~500 (≙100 µM EGTA) [43]	~500 (≙100 µM EGTA) [58]	n.d.	~1500 (≙300 µM BAPTA) [65]	~250 (≙50 µM Calbindin) [143] [l]

899

900

Abbreviations: AZ – active zone; hMFB – hippocampal mossy fiber bouton; FRP – fast releasing vesicle pool; SRP – slow releasing vesicle pool; n.d. – not determined.

[a] But see refs. [124, 144] for recordings from axon initial segment and axon 'blebs' of L5 pyramidal neurons, and ref. [145] for recordings from neocortical synaptosomes.

[b] But see ref. [142] for recordings from boutons of cultured hippocampal neurons and [146] for cell-attached recordings in hippocampal slice cultures.

[c] But a duration of 150 µs was also reported at the soma of neocortical pyramidal cells [14].

[d] Note that in lobule X, some mossy fibers have vesicular release probabilities ranging from 0.2–0.8 [147].

[e] The release probability of CA3 to CA3 synaptic connections is ~0.4 [148].

[f] Note that in contrast a recent study predicted an 'exclusion zone' separating vesicles and Ca^{2+} channels by at least 30 nm [149].

[g] Differential EGTA-sensitivity of synapses by layer 2/3 pyramidal cells onto two types of interneurons indicates target cell-specific difference of the coupling distance [66], but the high EGTA-sensitivity of release indicates large coupling distances in some excitatory neocortical neurons [66, 67].

[h] Note that this value is not well constrained, because the binominal *N* per cMFB-GC connection varies from 3–12 [68, 69, 126], the number of AZs per cMFB from 150–300 [32, 33, 116], and the number of GCs per cMFB from 12–50 [38, 116]. The mean across all these studies is: (*N* per connection)/((AZs per cMFB)/(GCs per cMFB)) = 7/(225/30) ≈ 1.

[i] Based on RRP of 53 (ref. [65]) and 25 AZ/hMFB [31]. Note that smaller estimates of RRP were obtained, ranging from 7 to 16 with 1.2 and 2.5 mM extracellular $[Ca^{2+}]$, respectively, which would result in an RRP/AZ < 1.

[j] Based on 15 fast and 7 slow releasable vesicles and the above mentioned values of AZs and GC connections, i.e. (15+7)/(225/30) = 3.

[k] Note that a rapid replenishment of fast releasing vesicles (FRP) from a pool of slowly releasing vesicles (SRP) was recently described (SDR, SRP-dependent recovery; ref. [150]), which has a rate constant in the range of 15 s^{-1} (E. Neher, personal communication).

Figures and figure legends

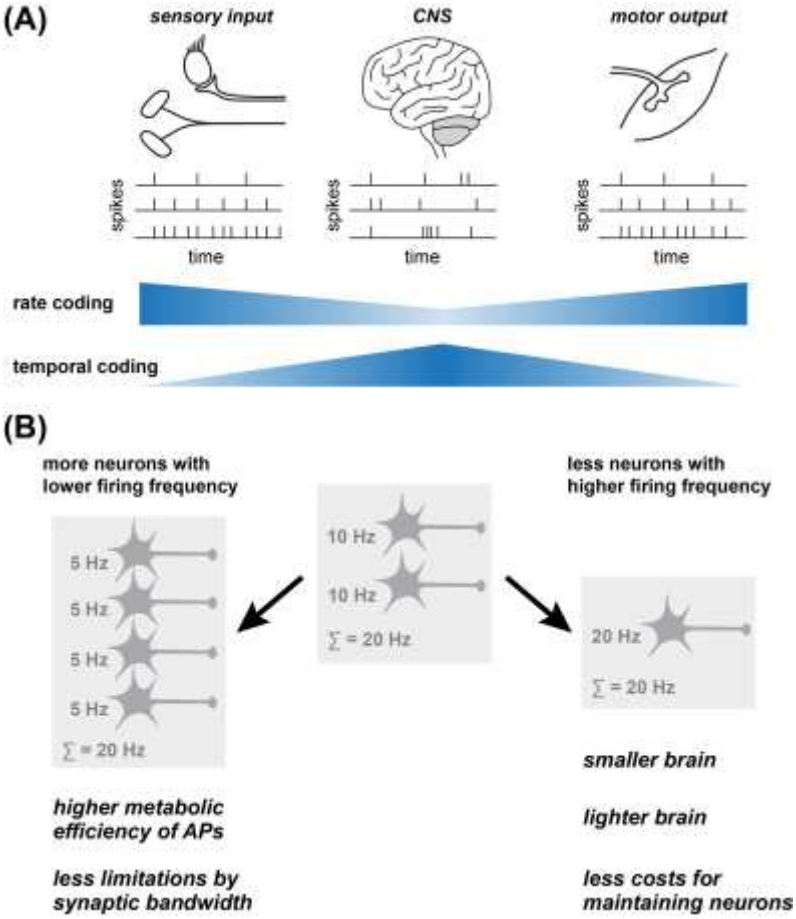

Figure 1: Evolutionary constrains for high-frequency rate coding

(A) Rate and temporal coding in the CNS and the input and output pathways. Whereas sensory information and motor commands are predominantly encoded via rate coding, temporal- and sparse coding becomes increasingly important in the CNS. **(B)** Illustration of three cell ensembles with different number of neurons and different respective average firing frequency. *Below:* Potential evolutionary advantages of the corresponding cell ensembles.

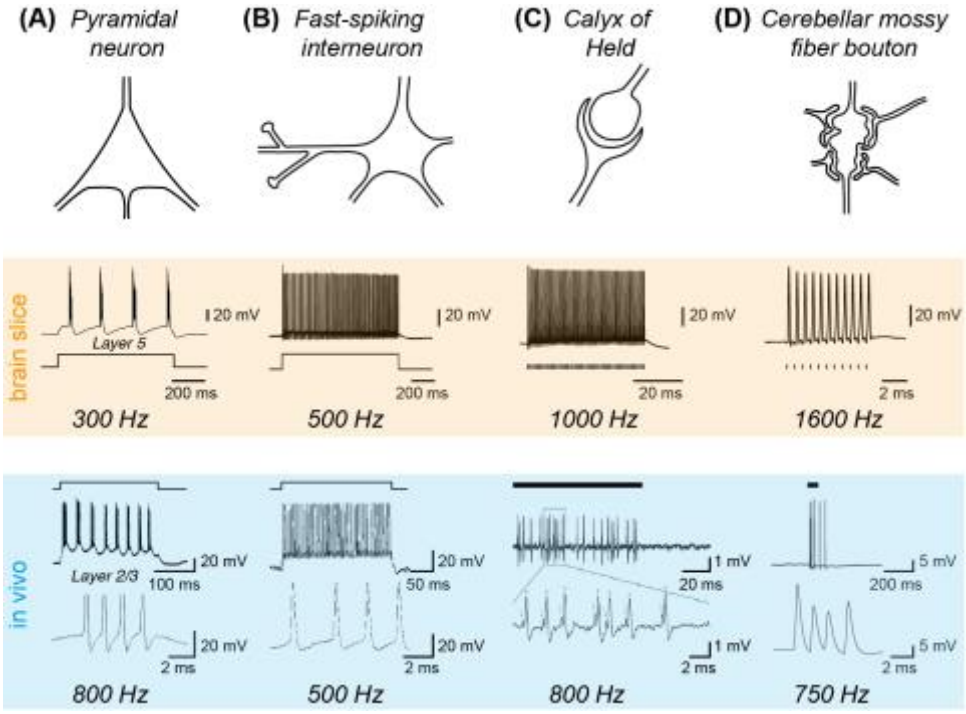

Figure 2. Evidence for high-frequency signaling in the mammalian CNS

Examples of recordings from high-frequency neurons and synapses in brain slices and *in vivo* with maximum instantaneous firing frequencies indicated (defined as the inverse of the shortest interval between APs). **(A)** Pyramidal neurons in the cerebral cortex can show typical burst firing, reaching several hundreds of Hertz within these bursts. Upper recording courtesy of M.H.P. Kole (data from ref. [108]), *in vivo* recording modified from ref. [14]. **(B)** Fast-spiking interneurons in the hippocampus or cerebral cortex display high AP frequencies with up to ~500 Hz. Upper recording modified from ref. [50], lower trace modified from ref. [16]. **(C)** The calyx of Held synapse conveying auditory information can reach Kilohertz frequencies. Upper recording modified from ref. [18], lower trace modified from ref. [19]. **(D)** Cerebellar mossy fibers and the presynaptic boutons may reach even higher AP frequencies. Upper recording modified from ref. [11], lower trace modified from ref. [22]. In brain slice recordings (orange shading), APs were elicited by current injection or axonal stimulation (indicated below the voltage traces). For the *in vivo* recordings (blue

shading), the stimulation is indicated above the voltage traces (current injection in A and B, tone in C, and air puff in D).

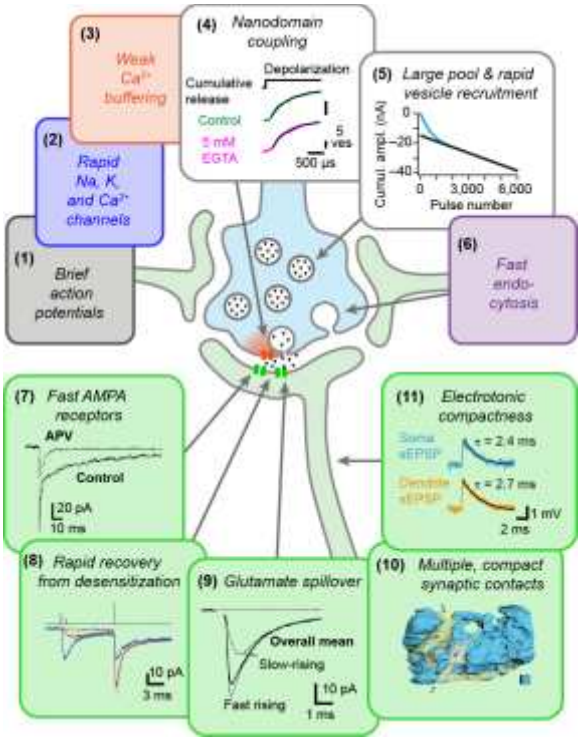

Figure 3. Mechanisms of high-frequency synaptic transmission

Summary of presynaptic (upper) and postsynaptic (lower) mechanisms supporting high-frequency synaptic transmission at the cMFB-GC synapse. The color code refers to corresponding traces in Figure 4. Data of panels 4, 5, and 7–11 are modified from refs. [42], [68], [34], [84], [85], [37], and [35], respectively.

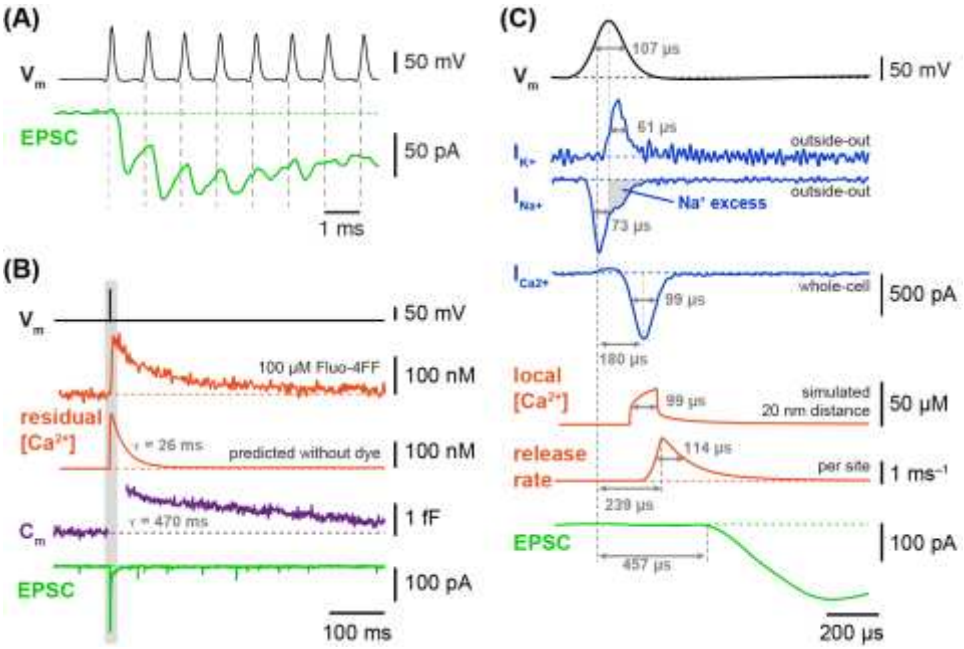

Figure 4. Rapid time course of synaptic transmission at the cMFB-GC synapse

(A) Paired recording from a cMFB (black) and GC (green) demonstrating reliable synaptic transmission at a frequency of 1 kHz (modified from ref. [11]). **(B)** Comparison of the time course of presynaptic AP (black, note consistent color-code in panel B and C), residual Ca^{2+} concentration (orange, *top:* measured with indicated Ca^{2+} indicator, *below:* simulated without Ca^{2+} indicator dye), endocytosis (purple), and EPSC (green). **(C)** Pre- and postsynaptic events on an expanded time scale. The very brief presynaptic AP (black) is mediated by fast K^+- and Na^+-currents (blue, upper), and evokes a rapid Ca^{2+}-current (blue, lower). The estimated local Ca^{2+} concentration and the release rate are illustrated in orange. The synchronous release of synaptic vesicles leads to an EPSC in the postsynaptic cell (green). Delays and half-widths are indicated; data are modified from refs. [11, 42, 43] and were aligned to the steepest rise of the presynaptic AP.

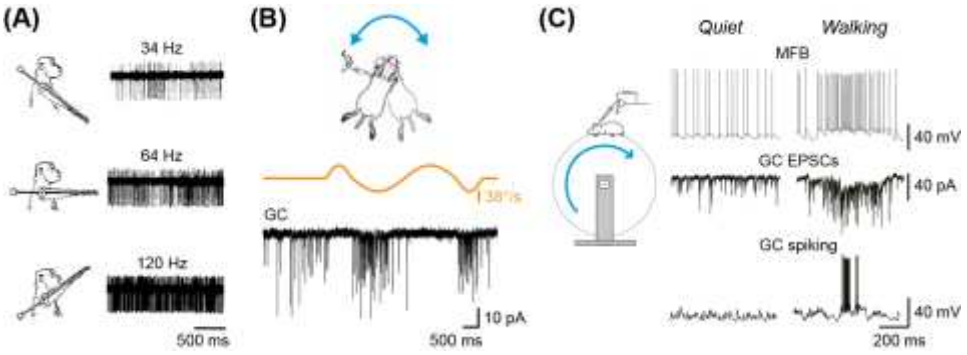

Figure 5. High-frequency coding at the cMFB-GC synapse in vivo

(A) Extracellular recordings from awake monkeys show that a joint angle is represented in the average firing frequency of mossy fibers. Modified from ref. [91]. **(B)** *In vivo* recording from anesthetized mice during horizontal rotation. Rotational velocity (orange) and recording of EPSCs in granule cells (black), indicating that mossy fibers linearly encode sensory information. Modified from ref. [93]. **(C)** Pre- and postsynaptic recordings from mice during locomotion. During walking, the firing frequency of mossy fibers increases (upper), leading to more EPSCs in granule cells (middle). The increased synaptic input from mossy fibers causes granule cell spiking during locomotion (lower). Modified from ref. [45].